IIETA International Information and Engineering Technology Association
Advancing the World of Information and Engineering

Traitement du Signal
Vol. 38, No. 4, August, 2021, pp. 1245-1251
Journal homepage: http://iieta.org/journals/ts

Impulse Noise Removal Based on Hybrid Genetic Algorithm

Nail Alaoui[1*], Arwa Mashat[2], Amel Baha Houda Adamou-Mitiche[1], Lahcène Mitiche[1], Aicha Djalab[3], Sara Daoudi[4], Lakhdar Bouhamla[1]

[1] Laboratoire de Recherche Modélisation, Simulation et Optimisation des Systèmes Complexes Réels, Université ZIANE Achour de Djelfa, Ain Chih, Djelfa 17000, Algeria
[2] Faculty of Computing & Information Technology, King Abdulaziz University, P.O. Box 344, Rabigh 21911, Saudi Arabia
[3] Department of Electrical Engineering, Faculty of Technology, University of Djelfa, P. O. B. 3117, Djelfa, Algeria
[4] RCAM Laboratory Dept of Electronics, Djillali Liabès University Sidi Bel Abbes, Sidi Bel Abbes 22000, Algeria

Corresponding Author Email: n.alaoui@univ-djelfa.dz

https://doi.org/10.18280/ts.380436

Received: 21 November 2020
Accepted: 12 July 2021

Keywords:
image denosing, noise removal, impulse noise, salt and pepper noise, genetic algorithm

ABSTRACT

In this paper, we introduce a new method, impulse noise removal based on hybrid genetic algorithm (INRHGA) to remove impulse noise at different noise densities of noise while preserving the main features of the image. The proposed approach merges the genetic algorithm and methods for filtering images that are combined into the population as essential solutions to create a developed and improved population. A set of individuals is developed into a number of iterations using factors of crossover and mutation. Our method develops a group of images instead of a set of parameters from the filters. We then introduced some of the concepts and steps of it. The proposed algorithm is compared with some image denoising algorithm. By using Peak Signal to Noise Ratio (PSNR), structural similarity (SSIM). For example, for Lenna image with 60% salt and pepper noise density, PSNR, SSIM results of AMF, MDBUTMFG and NAFSM methods are 20,39/ 28.74/ 29.85 and 0.5679/ 0.8312/ 0.8818 respectively, while PSNR, SSIM results of the proposed algorithm are 29.92 and 0.8838, respectively. Experimental results indicate that INRHGA is very effective and visually comparable with the above-mentioned methods at different levels of noise.

1. INTRODUCTION

Impulse noise removal is one of the essential issues in image processing, many approaches have been proposed to suppression of noise in digital images from the literature, and however, eliminate noise from digital images is still a difficult problem [1-7].

Different sensors, for example, laser scanners, medical scanners, cameras, and weather satellites, can obtain digital images, but these images might inherently be polluted by noise during acquisition compression processes, transmission [8-11]. It is essential to remove the noise while retaining the basic features of the image, such as edges and corners.

Some nonlinear filters have been suggested for the recuperation of images corrupted by impulse noise. The average filter, as well as its derivatives, are most common in image filtering.

The Median Filter (MF) method utilizes a fixed Window Size and is used to all pixels [12].

There are many common noise filters. For instance, the Adaptive Media Filter (AMF), which uses an adaptive window size, unlike MF which uses a fixed window size. However, although AMF is very effective at removing high-density Impulse noise in images compared to MF, but if the window size is large, it prevents us from finding pixels that match the pixels of the original image [13].

In high-density Impulse noise, a Modified Decision-Based Unsymmetrical Trimmed Median Filter (MDBUTMF) is used, where an adaptive window is used to identify and remove noisy pixels. Then, the MF is utilized to them [14]. Whereas Noise adaptive fuzzy switching median filter (NAFSM) applies the histogram to detect noise pixels in the noisy image, then these pixels are changed by applying MF or estimated according to their neighbors' values [15].

Other methods study the problem of removing noise from images as an optimization problem. Hence, genetic methods have been successfully applied. Some of the most modern papers involving genetic algorithms are [16-25].

Despite this interest, do not exist GAs intended to remove impulse noise in gray images by evolving images.

In this work, we describe a new genetic algorithm called INRHGA that removes impulse noise in gray images.

Our work is inspired by the approaches [19-21], but we address the problem from a different perspective. The fundamental idea is to merge the output images of two of the best methods found in the literature into the initial population of the Genetic Algorithm as essential solutions. Evolution happens for a certain number of epochs aiming to find the best image. During this process, a specific crossover and mutation are applied. Our method develops a group of images instead than a group of parameters from the filters. Our experimental results show that the proposed algorithm improves, in general, the performance for both image denoising and preservation of images details.

2. METHODOLOGIES

This section describes our proposed genetic algorithm that

suppresses noise in an image. The input of this proposed method is an image gray-scale N(x,y) perturbed through impulse noise. Enhanced image of N(x,y) is the output each individual in the proposed algorithm of the initial population is represented a denoised image of N(x,y).

In this paper, we employ the following two models for impulse noise in gray images:

i. Noise Model 1: Salt-and-pepper Impulse noise. For this model, the image is corrupted value by noise can only be 0 or 255 with the same probability.

The probability distribution function is given by:

$$f(x) = \begin{cases} \frac{p}{2} \text{ for } N = 0 \\ 1 - p \text{ for } N = O(i,j) \\ \frac{p}{2} \text{ for } N = 255 \end{cases} \quad (1)$$

where, p is the noise density in the image.

For each original image pixel at location (i; j) the intensity value is $O(i,j)$, the corresponding pixel of the noisy image is given by $N(i,j)$.

ii. Noise Model 2: For this model, Here corrupted image have fixed value for salt (i.e. 255) and pepper (i.e. 0) noise with unequal probability.

The probability distribution function is given by:

$$f(x) = \begin{cases} P_1 \text{ for } N = 0 \\ 1 - p \text{ for } N = O(i,j) \\ P_1 \text{ for } N = 255 \end{cases} \quad (2)$$

where, p = p1 + p2 is the noise density in the image and p1 ± p2.

Hybrid genetic algorithm is guided by the objective function expressed in Eq. (3).

$$ObjectFitness(F) = \lambda|I - N| + \left(\sum_{\Omega} \sqrt{1 + \beta^2 |\nabla I|^2}\right) \quad (3)$$

which is an edge aware feature preserving diffusion flow function stems from the studies [26, 27]. The term I(x,y) is the image being recovered, N(x,y) the noisy image, β and λ are balancing parameters and Ω is the set of all points in the image. where, $\lambda > 0$ and $1 \leq \beta \leq 2$ from [26].

By minimizing Eq. (1), we are basically trying to reduce the total variation of the image while preserving fidelity in relation to the original image.

The general execution for the proposed algorithm consists of the following steps:

INRHGA Algorithm Steps

Step 1. (Input image) Read a noisy image N(i,j) is represented by an array of pixels N(i,j) where i and j range from 0 to 255 and 255, respectively.

Step 2. (Initialization) Execute filters MDBUTMFG and NAFSM over noisy image N(i, j) to create two new images. $N_{MDBUTMFG}$ and N_{NAFSM}, respectively.

The first two individuals (images) of the population, denoted as $N_{MDBUTMFG}$, N_{NAFSM}, are the resulting images after applying the following filters: MDBUTMFG and NAFSM to noisy images (Input image)

Then, execute a pixel recombination procedure that randomly exchanges pixels between $N_{MDBUTMFG}$ and N_{NAFSM} to create an initial population of size Ps.

Step 3. (Evaluation) Use Eq. (1) to evaluate the fitness of the initial population.

Step 4. (Selection) Select a pair of the initial population by a Roulette Wheel selection.

Step 5. (Crossover) crossing pairs of selected parents to create offspring. We have applied the same crossover factors proposed by Ahmed and Das [4].

Step 6. (Mutation) Mutate each offspring with probability P_m through the execution of one of the filters MDBUTMFG or NAFSM selected randomly.

Step 7. (Update population) Choose the best Ps individuals of previous generation and their offspring according to their fitness, then retain these individuals for the next iteration as an initial population.

Step 8. Steps 3 to 7 are repeated until $iter_{max}$ is reached.

The best individual according to the fitness value in the last generation is considered as the denoised image I(i,j).

This configuration was based on some empirical tests that took into account the computational time spent by executing the INRHGA combined with the other denoising methods. For example, it is not possible to set a large-sized population since it makes initialization and mutation processes very time-consuming.

Table 1. Configuration set for the impulse noise removal based on hybrid genetic algorithm

Size of the population (P_s)	30
Mutation rate (P_m)	0.02
Completion-criteria ($iter_{max}$) number of iterations	when the algorithm reaches = 20 generations
β	1
λ	0.08
Selection criteria	Roulette Wheel selection

Table 1 shows the parameter settings for the proposed algorithm. We selected the values of these parameters by performing initial experiments taking into account the trade-off between time and efficiency

3. EXPERIMENTAL RESULTS

In this section, we first presented six test images exposed. The first four of these images are among the most popular images. The second two of them are from TEST IMAGES [5, 28], as Figure 1 and Figure 2 shown, respectively.

Figure 3 and Figure 4 give the results of AMF, MDBUTMF, NAFSMF, and INRHGA for Girl face and Chair image with 80% and 90 % densities by model 1 and model 2 of impulse noise, respectively. INRHGA preserved better the details of the image compared to other methods.

Moreover, Figure 5 and Figure 6 illustrates the results of INRHGA considering the input image Lenna and Billiard-Ball with noise densities (20%, 40%, 60%, 80% and 90%) by model 1 and 2 of impulse noise, respectively

Afterwards, in Tables 2 and 3, we give results PSNR and SSIM of the methods of model 1, for Bridge, Couple, Girl face, and Lenna images ranging in noise densities from 10% to 90%. Moreover, in Tables 4 and 5, we give the results PSNR and SSIM of the methods of model 2 for the same as test images. The results show that INRHGA performs better than the others at all noise densities in model 1 above 10% and all noise densities in model 2 above 30%.

Peak signal to noise ratio (PSNR) is defined as:

$$PSNR = 10 \cdot log\left(\frac{255^2}{MSE}\right) \quad (4)$$

where, MSE (Mean Square Error) is defined as:

$$MSE = \frac{1}{M \times N}\sum_{i=0}^{M-1}\sum_{j=0}^{N-1}[O(i,j) - I(i,j)]^2 \quad (5)$$

where, O(i,j) and I(i,j) are the original image and the recovered image, respectively. Where M and N are the image dimensions.

Structural similarity index metric (SSIM), which can be mathematically formulated [6, 29], is defined as:

$$SSIM(x,y) = \frac{(2\mu_x\mu_y + c_1)(2\sigma_{xy} + c_2)}{(\mu_x^2 + \mu_y^2 + c_1)(\sigma_x^2 + \sigma_y^2 + c_2)} \quad (6)$$

where, μ_x, μ_y, σ_x^2, σ_y^2, $and\ \sigma_{xy}$ are the mean intensities, standard deviations and covariance for images x and y, respectively. $c_1 = (k_1 L)^2$ and $c_2 = (k_2 L)^2$ that L = 255 for 8-bit grayscale images and k_1=0.01 and k_2=0.03 are constant.

(a) Lenna (b) Couple (c) Bridge (d) Girlface

Figure 1. Classic test images

(a) Billiard-Ball (b) Chair

Figure 2. TESTIMAGES Database

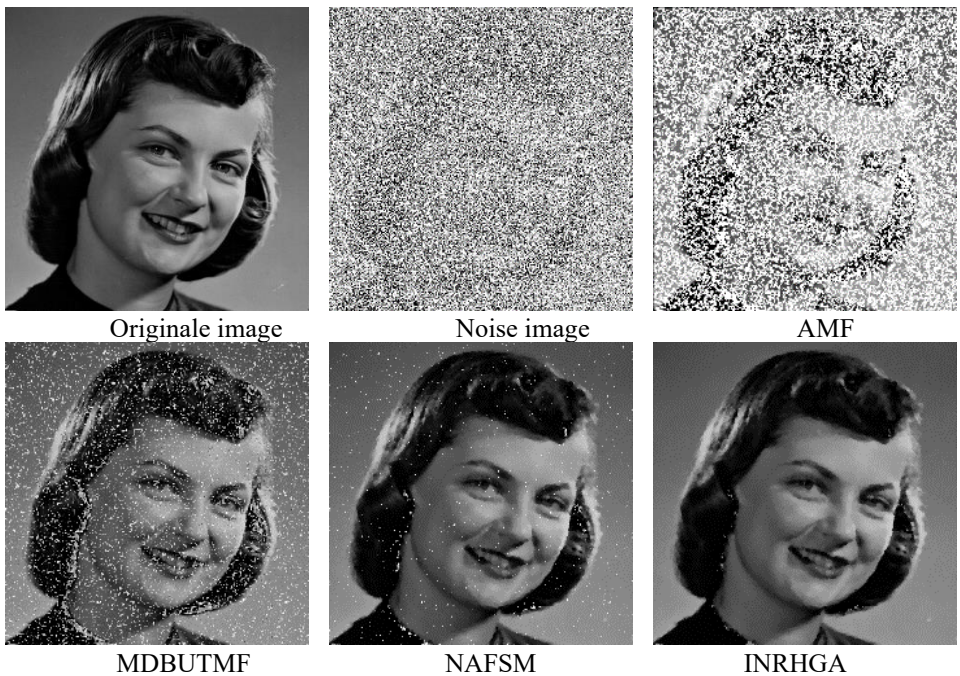

Originale image Noise image AMF

MDBUTMF NAFSM INRHGA

Figure 3. Restoration results of Girlface image perturbed by model 1 impulse noise with 80% densities

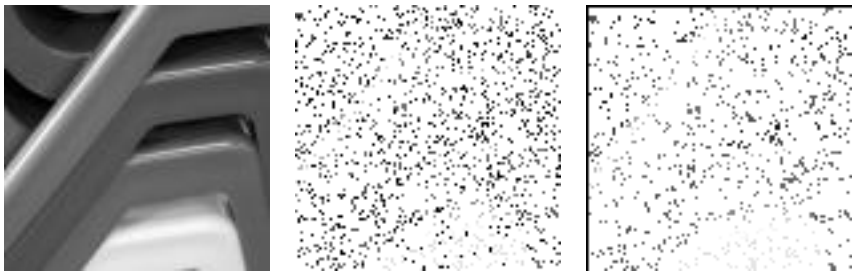

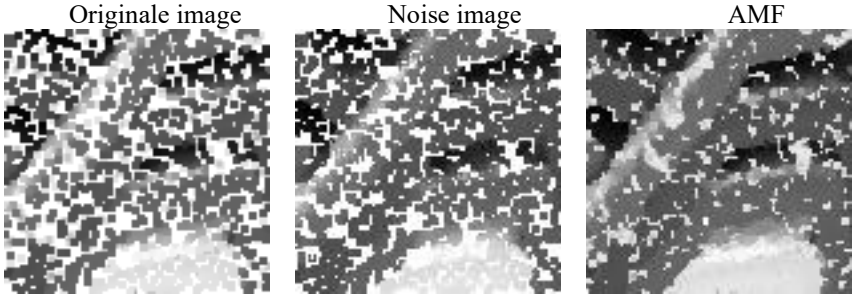

Figure 4. Restoration results of chair image perturbed by model 2 impulse noise with 90% densities

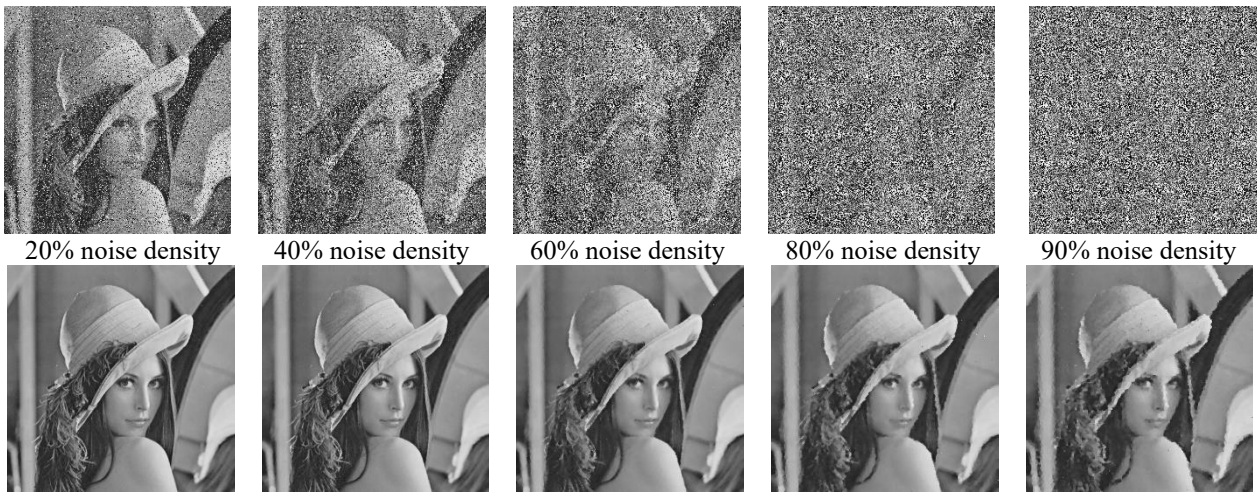

Figure 5. Lenna perturbed by impulse noise of model 1, and Lenna images after INRHGA

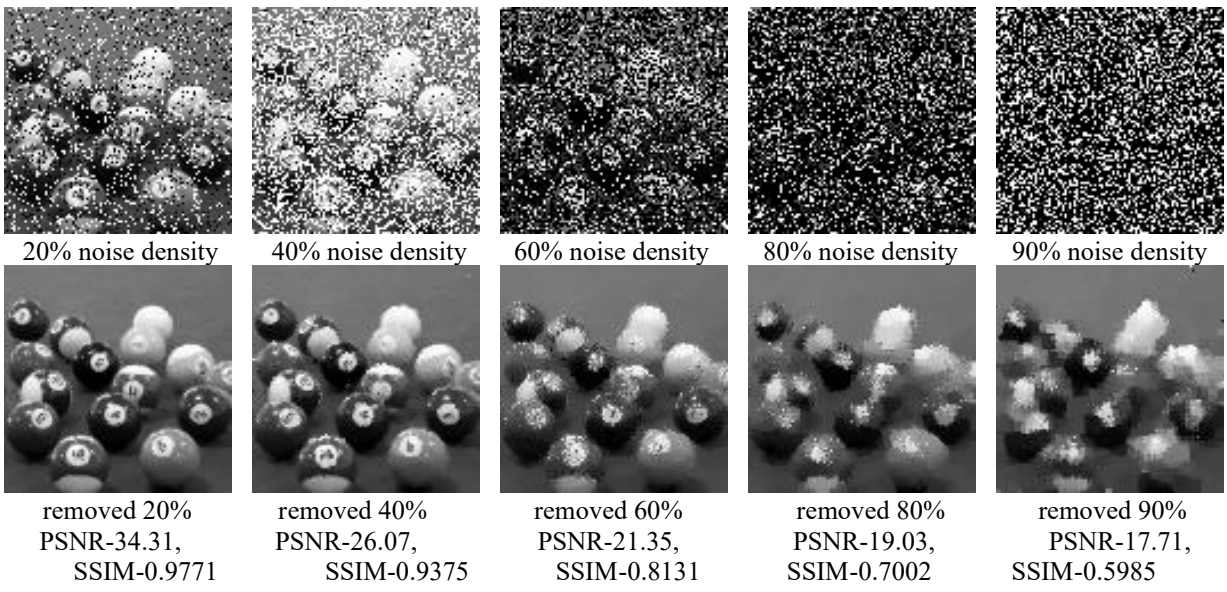

Figure 6. Billiard-Ball perturbed by impulse noise of model 2, and Billiard-Ball images after INRHGA

Table 2. PSNR results in the methods of model 1 for some images

Image	Filter	10%	20%	30%	40%	50%	60%	70%	80%	90%
Bridge	AMF	20,1999	20,1086	19,9944	19,849	19,373	17,8678	15,0618	11,577	8,1826
	MDBUTMF	34,1312	31,0621	28,6614	26,9952	25,454	23,5619	21,1819	18,1645	14,6439
	NAFSM	31,4271	28,6628	26,8445	25,5179	24,4377	23,4427	22,582	21,472	19,5182
	INRHGA	33,9909	30,8605	28,8919	27,0549	25,4826	23,6082	22,6709	21,7622	20,3202
Couple	AMF	22,4939	22,4284	22,332	22,1433	21,5342	19,5363	15,9518	12,0989	8,578
	MDBUTMF	38,5303	35,1063	32,6023	30,7843	27,2103	26,2491	23,5481	19,8943	16,0675
	NAFSM	34,3544	31,5208	29,5767	28,3064	27,1942	26,2143	25,2502	24,1182	21,5846
	INRHGA	38,5815	35,1237	32,6975	30,8103	28,9488	26,6344	25,3306	24,3105	22,873
Girlface	AMF	25,8914	25,8499	25,7482	25,4966	24,0687	20,5702	15,9459	11,7346	7,973
	MDBUTMF	38,8938	34,7307	32,9888	30,2575	27,9465	25,098	21,529	17,6643	13,7966
	NAFSM	37,7447	35,0151	33,3937	31,9485	30,985	29,7196	27,9988	26,031	21,8677
	INRHGA	38,9201	35,399	33,6443	32,2003	31,0969	30,1319	28,0003	27,4157	24,7181
Lenna	AMF	24,4338	24,3768	24,2976	24,0807	22,9636	20,3858	16,4434	12,1157	8,4666
	MDBUTMF	42,9759	39,0355	36,6427	34,6372	31,0664	28,7388	24,7712	20,1186	15,8785
	NAFSM	38,8213	35,6225	33,7468	32,323	31,0581	29,8547	28,639	27,0991	23,5366
	INRHGA	42,9204	39,2671	36,7048	34,6952	32,1341	29,9186	28,7633	27,4698	23,4983
Mean	AMF	23,2548	23,1910	23,0931	22,8924	21,9849	19,5900	15,8507	11,8816	08,3000
	MDBUTMF	38,6328	34,9837	32,7238	30,6686	27,9193	25,9120	22,7576	18,9604	15,0966
	NAFSM	35,5869	32,7053	30,8904	29,5240	28,4188	27,3079	26,1175	24,6801	21,6268
	INRHGA	38,6032	35,1626	32,9846	31,1902	29,4156	27,5733	26,1913	25,2396	22,8524

Table 3. SSIM results in the methods of model 1 for some images

Image	Filter	10%	20%	30%	40%	50%	60%	70%	80%	90%
Bridge	AMF	0,4901	0,4823	0,4765	0,4698	0,4477	0,3857	0,2663	0,1242	0,0386
	MDBUTMF	0,9789	0,9535	0,9208	0,8839	0,8348	0,7194	0,6147	0,4207	0,2037
	NAFSM	0,9622	0,9225	0,8774	0,8311	0,778	0,7185	0,6483	0,5678	0,4337
	INRHGA	0,978	0,9528	0,9224	0,8857	0,8354	0,7536	0,6523	0,5731	0,4556
Couple	AMF	0,6086	0,6028	0,5974	0,5881	0,5614	0,4694	0,291	0,1146	0,0353
	MDBUTMF	0,9865	0,9682	0,9446	0,9164	0,8514	0,7889	0,6556	0,4283	0,2031
	NAFSM	0,9715	0,941	0,9065	0,8712	0,8318	0,7872	0,735	0,6642	0,5328
	INRHGA	0,9868	0,9684	0,9456	0,9173	0,8754	0,7978	0,7372	0,674	0,5785
Girlface	AMF	0,8117	0,8068	0,8015	0,7926	0,7425	0,6065	0,3393	0,1197	0,0307
	MDBUTMF	0,9788	0,9643	0,9481	0,9295	0,8888	0,7925	0,5933	0,3292	0,1289
	NAFSM	0,9808	0,9636	0,9488	0,9305	0,9133	0,8919	0,8642	0,8258	0,7048
	INRHGA	0,9797	0,9651	0,9499	0,9308	0,9128	0,8925	0,8643	0,8398	0,7655
Lenna	AMF	0,7606	0,7544	0,7501	0,739	0,6941	0,5679	0,3325	0,116	0,0308
	MDBUTMF	0,9923	0,9805	0,9671	0,9486	0,9081	0,8312	0,6622	0,3982	0,17
	NAFSM	0,9859	0,9684	0,9504	0,9304	0,9078	0,8818	0,8511	0,8017	0,6819
	INRHGA	0,9922	0,9806	0,9671	0,9486	0,9141	0,8838	0,8546	0,8145	0,6843
Mean	AMF	0,6678	0,6616	0,6564	0,6474	0,6114	0,5074	0,3073	0,1186	0,0339
	MDBUTMF	0,9841	0,9666	0,9452	0,9196	0,8708	0,7830	0,6315	0,3941	0,1764
	NAFSM	0,9751	0,9489	0,9208	0,8908	0,8577	0,8199	0,7747	0,7149	0,5883
	INRHGA	0,9842	0,9667	0,9463	0,9206	0,8844	0,8319	0,7771	0,7254	0,6210

Table 4. PSNR results in the methods of model 2 for some images

Image	Filter	10%	20%	30%	40%	50%	60%	70%	80%	90%
Bridge	AMF	20,2292	20,1175	19,7925	19,7336	15,5264	12,2532	8,3407	8,1846	8,2234
	MDBUTMF	34,2978	30,9631	28,4768	27,2498	24,7438	23,3324	19,1457	17,194	14,686
	NAFSM	31,6324	28,6236	27,1551	25,668	24,6961	23,3968	21,3106	20,4548	19,576
	INRHGA	34,2485	31,1783	29,1414	27,4299	25,6565	23,4906	22,6891	21,9699	20,2707
Couple	AMF	22,4913	22,3805	21,6792	21,4383	21,5016	9,7861	14,3058	6,4795	7,7111
	MDBUTMF	38,8286	34,9707	32,6247	30,6118	27,1889	24,2666	23,225	15,3942	15,3997
	NAFSM	34,6116	31,4578	29,5988	28,2863	27,2266	24,7258	25,229	18,2933	20,9087
	INRHGA	38,6923	35,0506	32,6346	30,8723	28,9528	26,2601	25,3163	24,2971	22,7802
Girlface	AMF	25,9081	25,7956	24,3552	21,4275	12,3631	8,3342	15,18	12,6008	8,9335
	MDBUTMF	40,9269	39,2026	36,7941	27,8005	24,3342	20,9944	23,3093	19,1281	15,0042
	NAFSM	37,9844	35,763	33,9727	31,4295	28,8787	26,044	28,4429	26,3813	19,1511
	INRHGA	37,2819	38,2856	33,6955	31,9982	31,3146	29,8498	28,5719	28,1635	24,5959
Lenna	AMF	24,4611	24,3632	24,2775	23,6891	21,7659	17,15	16,1279	6,3904	5,7879
	MDBUTMF	42,9293	39,1671	36,761	34,501	30,942	28,4891	24,5797	15,0837	11,1496
	NAFSM	38,7396	35,5846	33,7161	32,3598	30,8756	29,6132	28,6649	17,3033	14,2669
	INRHGA	42,7286	39,1743	36,7786	34,6075	31,9927	29,9361	28,7636	27,4954	25,3531
Mean	AMF	23,2724	23,1642	22,5261	21,5721	17,7893	11,8809	13,4886	8,4138	7,6640
	MDBUTMF	39,2457	36,0759	33,6642	30,0408	26,8022	24,2706	22,5649	16,7000	14,0599
	NAFSM	35,7420	32,8573	31,1107	29,4359	27,9193	25,9450	25,9119	20,6082	18,4757
	INRHGA	38,2378	35,9222	33,0625	31,2270	29,4792	27,3842	26,3352	25,4815	23,2500

Table 5. SSIM results in the methods of model 2 for four some images

Image	Filter	10%	20%	30%	40%	50%	60%	70%	80%	90%
Bridge	AMF	0,4917	0,4824	0,4711	0,4638	0,2959	0,1634	0,0847	0,0486	0,0426
	MDBUTMF	0,9785	0,9519	0,9218	0,885	0,8186	0,7191	0,5615	0,4037	0,2056
	NAFSM	0,9618	0,9207	0,8781	0,8303	0,7762	0,7041	0,6161	0,5025	0,4365
	INRHGA	0,979	0,9529	0,9212	0,8832	0,8306	0,7369	0,6513	0,5723	0,4534
Couple	AMF	0,6087	0,6044	0,5766	0,5623	0,5584	0,0729	0,2346	0,0357	0,0288
	MDBUTMF	0,9869	0,9675	0,9447	0,9149	0,8307	0,7413	0,6424	0,2798	0,1874
	NAFSM	0,9726	0,9407	0,9066	0,8711	0,8322	0,7366	0,731	0,3968	0,4899
	INRHGA	0,9871	0,968	0,9451	0,9182	0,875	0,7876	0,737	0,6733	0,5769
Girlface	AMF	0,8127	0,8078	0,746	0,6806	0,2095	0,055	0,2848	0,1653	0,0887
	MDBUTMF	0,9843	0,9805	0,948	0,9232	0,8676	0,716	0,6253	0,3541	0,1481
	NAFSM	0,9812	0,9645	0,9454	0,9295	0,8991	0,8341	0,854	0,8068	0,405
	INRHGA	0,9798	0,9738	0,9667	0,9314	0,9115	0,8935	0,8665	0,8272	0,767
Lenna	AMF	0,7624	0,7558	0,7488	0,729	0,6417	0,4009	0,3239	0,0419	0,0662
	MDBUTMF	0,9923	0,9804	0,967	0,9476	0,908	0,8269	0,6542	0,2452	0,1013
	NAFSM	0,9859	0,9682	0,9502	0,9304	0,9066	0,8788	0,8497	0,352	0,1874
	INRHGA	0,9919	0,9804	0,9671	0,9484	0,9136	0,8837	0,8535	0,816	0,7443
Mean	AMF	0,6689	0,6626	0,6356	0,6089	0,4264	0,1731	0,2320	0,0729	0,0566
	MDBUTMF	0,9855	0,9701	0,9454	0,9177	0,8562	0,7508	0,6209	0,3207	0,1606
	NAFSM	0,9754	0,9485	0,9201	0,8903	0,8535	0,7884	0,7627	0,5145	0,3797
	INRHGA	0,9845	0,9688	0,9500	0,9203	0,8827	0,8254	0,7771	0,7222	0,6354

4. CONCLUSIONS

In this paper, we have proposed a new impulse noise removal by applying a hybrid genetic algorithm (INRHGA), we address the reduction of impulse noise in images as an optimization problem, which gives better performance in comparison with known noise removal methods in terms of PSNR and SSIM. The performance of the algorithm has been tested an all noise densities on grayscale images. The proposed method is effective for impulse noise removal. An important advantage of INRHGA is impulse noise removal in noisy image without the original image, so it works without a clue about how far we are from the original image.

Finally, our scope of work did not focus on the arithmetic cost of the algorithm, but on the quality of the recovered images. We intend to verify the computational cost and reduce the current implementation time of the proposed algorithm as future work.

REFERENCES

[1] Fareed, S.B.S., Khader, S.S. (2018). Fast adaptive and selective mean filter for the removal of high-density salt and pepper noise. IET Image Processing, 12(8): 1378-1387.

[2] Chen, J., Zhan, Y., Cao, H., Wu, X. (2018). Adaptive probability filter for removing salt and pepper noises. IET Image Processing, 12(6): 863-871.

[3] Mafi, M., Tabarestani, S., Cabrerizo, M., Barreto, A., Adjouadi, M. (2018). Denoising of ultrasound images affected by combined speckle and Gaussian noise. IET Image Processing, 12(12): 2346-2351.

[4] Ahmed, F., Das, S. (2013). Removal of high-density salt-and-pepper noise in images with an iterative adaptive fuzzy filter using alpha-trimmed mean. IEEE Transactions on Fuzzy Systems, 22(5): 1352-1358. https://doi.org/10.1109/TFUZZ.2013.2286634

[5] Erkan, U., Gökrem, L., Enginoğlu, S. (2019). Adaptive right median filter for salt-and-pepper noise removal. International Journal of Engineering Research and Development, 11(2): 542-550. https://doi.org/10.29137/umagd.495904

[6] Thanh, D.N.H., Engínoğlu, S. (2019). An iterative mean filter for image denoising. IEEE Access, 7: 167847-167859. https://doi.org/10.1109/ACCESS.2019.2953924

[7] Erkan, U., Gökrem, L., Enginoğlu, S. (2018). Different applied median filter in salt and pepper noise. Computers & Electrical Engineering, 70: 789-798. https://doi.org/10.1016/j.compeleceng.2018.01.019

[8] Abdurrazzaq, A., Mohd, I., Junoh, A.K., Yahya, Z. (2018). Modified tropical algebra based median filter for removing salt and pepper noise in digital image. IET Image Processing, 13(14): 2790-2795. https://doi.org/10.1049/iet-ipr.2018.6201

[9] Chen, J., Zhan, Y., Cao, H., Xiong, G. (2019). Iterative grouping median filter for removal of fixed value impulse noise. IET Image Processing, 13(6): 946-953.

[10] Naimi, H., Adamou-Mitiche, A.B.H., Mitiche, L. (2015). Medical image denoising using dual tree complex thresholding wavelet transform and Wiener filter. Journal of King Saud University-Computer and Information Sciences, 27(1): 40-45. https://doi.org/10.1016/j.jksuci.2014.03.015

[11] Lone, A.H., Siddiqui, A.N. (2018). Noise models in digital image processing. Global Sci-Tech, 10(2): 63-66. https://doi.org/10.5958/2455-7110.2018.00010.1

[12] Bovik, A.C. (2010). Handbook of Image and Video Processing. Academic Press. 2005, p. vii.

[13] Hwang, H., Haddad, R.A. (1995). Adaptive median filters: New algorithms and results. IEEE Transactions on Image Processing, 4(4): 499-502. https://doi.org/10.1109/83.370679

[14] Pattnaik, A., Agarwal, S., Chand, S. (2012). A new and efficient method for removal of high density salt and pepper noise through cascade decision based filtering algorithm. Procedia Technology, 6: 108-117. https://doi.org/10.1016/j.protcy.2012.10.014

[15] Toh, K.K.V., Isa, N.A.M. (2009). Noise adaptive fuzzy switching median filter for salt-and-pepper noise reduction. IEEE Signal Processing Letters, 17(3): 281-

284. https://doi.org/10.1109/LSP.2009.2038769
[16] Toledo, C.F., de Oliveira, L., da Silva, R.D., Pedrini, H. (2013). Image denoising based on genetic algorithm. In 2013 IEEE Congress on Evolutionary Computation, pp. 1294-1301. https://doi.org/10.1109/CEC.2013.6557714
[17] de Paiva, J.L., Toledo, C.F., Pedrini, H. (2015). A hybrid genetic algorithm for image denoising. In 2015 IEEE Congress on Evolutionary Computation (CEC), pp. 2444-2451. https://doi.org/10.1109/CEC.2015.7257188
[18] Sakthidasan, K., Nagappan, N.V. (2016). Noise free image restoration using hybrid filter with adaptive genetic algorithm. Computers & Electrical Engineering, 54: 382-392. https://doi.org/10.1016/j.compeleceng.2015.12.011
[19] Fajardo-Delgado, D., Sánchez, M.G., Molinar-Solis, J.E., Fernandez-Zepeda, J.A., Vidal, V., Verdiú, G. (2016). A hybrid genetic algorithm for color image denoising. In 2016 IEEE Congress on Evolutionary Computation (CEC), pp. 3879-3886. https://doi.org/10.1109/CEC.2016.7744281
[20] de Paiva, J.L., Toledo, C.F., Pedrini, H. (2016). An approach based on hybrid genetic algorithm applied to image denoising problem. Applied Soft Computing, 46: 778-791. https://doi.org/10.1016/j.asoc.2015.09.013
[21] Sánchez, M.G., Fajardo-Delgado, D., Vidal, V., Verdú, G. (2020). A hybrid genetic algorithm to reduce the radiation dose in CR images. Radiation Physics and Chemistry, 167: 108275. https://doi.org/10.1016/j.radphyschem.2019.04.025
[22] Alaoui, N., Adamou-Mitiche, A.B.H., Mitiche, L. (2020). Effective hybrid genetic algorithm for removing salt and pepper noise. IET Image Processing, 14(2): 289-296.
[23] Saraiva, A.A., de Oliveira, M.S., de Moura Oliveira, P. B., Solteiro Pires, E.J., Fonseca Ferreira, N.M., Valente, A. (2019). Genetic algorithm applied to remove noise in DICOM images. Journal of Information and Optimization Sciences, 40(7): 1543-1558. https://doi.org/10.1080/02522667.2019.1597999
[24] Verma, D., Vishwakarma, V.P., Dalal, S. (2020). A hybrid self-constrained genetic algorithm (HSGA) for digital image Denoising based on PSNR improvement. In Advances in Bioinformatics, Multimedia, and Electronics Circuits and Signals, 1064: 135-153. Springer, Singapore. https://doi.org/10.1007/978-981-15-0339-9_12
[25] Shen, C., Wang, D., Tang, S., Cao, H., Liu, J. (2017). Hybrid image noise reduction algorithm based on genetic ant colony and PCNN. The Visual Computer, 33(11): 1373-1384. https://doi.org/10.1007/s00371-016-1325-x
[26] Zosso, D., Bustin, A. (2014). A primal-dual projected gradient algorithm for efficient Beltrami regularization. Computer Vision and Image Understanding, 14-52.
[27] Chan, T.F., Esedoglu, S. (2005). Aspects of total variation regularized L 1 function approximation. SIAM Journal on Applied Mathematics, 65(5): 1817-1837. https://doi.org/10.1137/040604297
[28] Asuni, N., Giachetti, A. (2014, September). TESTIMAGES: A Large-scale Archive for Testing Visual Devices and Basic Image Processing Algorithms. In STAG, 63-70.
[29] Wang, Z., Bovik, A.C., Sheikh, H.R., Simoncelli, E.P. (2004). Image quality assessment: From error visibility to structural similarity. IEEE Transactions on Image Processing, 13(4): 600-612. https://doi.org/10.1109/TIP.2003.819861